Available on CMS information server

CMS NOTE 2006-068

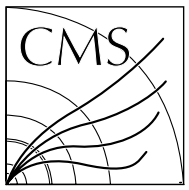

The Compact Muon Solenoid Experiment

CMS Note

Mailing address: CMS CERN, CH-1211 GENEVA 23, Switzerland

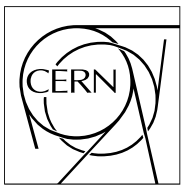

October 14th 2006

Study of PDF and QCD scale uncertainties in $\mathrm{pp} \to \mathrm{ZZ} \to 4\mu$ events at the LHC

S. Abdullin[a], P. Bartalini[b], R. Cavanaugh[b], A. Drozdetskiy[b], A. Korytov[b], G. Mitselmakher[b], Yu. Pakhotin[b], B. Scurlock[b], A. Sherstnev[c], H. Stenzel[d]

a: Fermi National Laboratory, Chicago, IL, USA

b: University of Florida, FL, USA

c: Moscow State University, Russia

d: Justus-Liebig Universität, Giessen, Germany

Abstract

Theoretical uncertainties from Parton Distribution Functions and from renormalization and factorization scales are studied for the $\mathrm{q\bar{q}} \to \mathrm{ZZ} \to 4\mu$ process, the main irreducible background in searches for the Higgs boson via its $\mathrm{H} \to \mathrm{ZZ} \to 4\mu$ decay mode. Effects are quoted for both total and differential cross sections, investigating the distributions used in the $\mathrm{pp} \to \mathrm{H} \to 4\mu$ search. An experimental methodology for the normalization to "side-bands" and to the single Z boson production cross section is proposed.

1 introduction

The $q\bar{q} \to ZZ \to 4\mu$ process is the main irreducible background in searches for the Higgs boson via its $H \to ZZ \to 4\mu$ decay mode. Theoretical uncertainties affect the current estimation of the physics reach for the search analysis and may turn into contributions to the total systematic errors on significance estimators, as background evaluation on a specific 4-muon mass range often relies on extrapolations from regions with larger background statistics, which are based on Monte Carlo Models. Normalization to higher rate processes like single Z production may help to reduce these uncertainties. This work concentrates on the estimation of the errors in the calculations of the total and differential cross sections for the process $q\bar{q} \to ZZ \to 4\mu$, which are arising from PDF and perturbative uncertainties. The error analysis relies on the guidelines described in [1] for the evaluation of theoretical uncertainties in CMS analyses.

2 Event Generation

All the results are obtained at NLO with MCFM [2] version 4.0 interfaced to the standard Les Houches accord PDF package LHAPDF [3]. The cross sections are evaluated within a typical experimental acceptance and for momentum cuts summarized in Section 3. The calculations with MCFM are carried out for the default set of electroweak input parameters (corresponding to the MCFM setting EWSCHEME=-1) using the effective field theory approach. $q\bar{q} \to ZZ \to 4\mu$ events are simulated adopting MCFM process number 81 ($q\bar{q} \to ZZ \to \mu^+\mu^-e^+e^-$), i.e. neglecting the interference between the propagators. The PDF family CTEQ61 provided by the CTEQ collaboration [4] is taken as nominal PDF input. A quantitative error analysis is performed following the prescription of reference [5] using the 40 sets of CTEQ61. Errors are propagated via re-weighting to the final observables. MRST2001E given by the MRST group [6] is considered as an additional cross check. The value of the strong coupling α_s is not a free input parameter for the cross section calculation but taken from the corresponding value in the PDF set.

The dependence of the observables on the choice for renormalization and factorization scales is unphysical and should be regarded as one important contribution to the total uncertainty in the theoretical predictions accounting for missing higher orders in QCD calculations. The reference cross sections and distributions are obtained with $\mu_R = \mu_F = 2M_Z$. Missing higher orders are estimated by independent variations of the two scales in the range $M_Z < \mu < 4M_Z$, following prescriptions applied to other processes [7].

3 Definition of observables and event selection

In order to perform a generator-level study with MCFM, we select events fulfilling acceptance and momentum cuts very much along the lines of the ones optimized for the full simulation-level mass dependent analysis [8]. General pre-selection cuts and three different sets of selection cuts are defined, the latter being driven by the Higgs search in four muon final states at "Low", "Average" and "High" Higgs masses (M_H = 150, 250, and 500 GeV respectively).

The pre-selection cuts are:

- There should be at least four muons (2 opposite sign muon pairs) for an event to be considered.

Table 1: Relative uncertainty on the total cross section $\sigma(q\bar{q} \to ZZ \to 4\mu)$ with pre-selection cuts and on $d\sigma/dM(4\mu)$ evaluated for three values of $M(4\mu)$ with selection cuts. Reference figures correspond to the CTEQ61 PDF set and $\mu_F = \mu_R = 2M_Z$. Asymmetric errors arising from the choice of the QCD scales are obtained adopting independent variations of μ_F and μ_R in the range $M_Z < \mu < 4M_Z$. Symmetric errors from PDF parameterization are obtained using the CTEQ61 error sets. Differences in the predictions with respect to the reference MRST2001E set are also reported.

	$\Delta(\sigma)$	$\Delta(d\sigma/dM(4\mu))$	$\Delta(d\sigma/dM(4\mu))$	$\Delta(d\sigma/dM(4\mu))$
	(pre-selection cuts)	(M_H=150 GeV)	(M_H=250 GeV)	(M_H=500 GeV)
μ_F and μ_R scales	+3.2% -4.0%	+2.3% -4.4%	+3.4% -4.3%	+3.8% -2.5%
PDF (CTEQ61)	±4.8%	±5.1%	±4.7%	±4.4%
Δ(MRST2001E)	+4.6%	+0.4%	+4.8%	+6.6%

- $P_T > 7$ GeV for all the four muons.
- Opposite sign muon pairs arising from Z/γ decays should have invariant mass $M_{\mu^+\mu^-} > 12$ GeV. This cut on $M_{\mu^+\mu^-}$ removes low-mass resonances.

The selection cuts are obtained from the pre-selection cuts, increasing the lower P_T threshold on the four muons to 10, 16 and 25 GeV for $M_H = 150$, 250, and 500 GeV respectively.

The notations that we use in this work include:

- $M(4\mu)$ is the invariant mass of the four selected muons.
- $P_T(4\mu)$ is the transverse momentum of the four muons system.
- Z1 refers to the muon pair with invariant mass closest to the Z mass and Z2 refers to the second muon pair selected from the rest of the muons with the highest P_T.

4 Study of uncertainties from PDF and QCD scales

The total effective cross section $\sigma(q\bar{q} \to ZZ \to 4\mu)$ with pre-selection cuts for the CTEQ61 PDF set and $\mu_F = \mu_R = 2M_Z$ turns out to be 18.6 fb. The $M(4\mu)$ distribution is given in Fig. 1, along with uncertainties from the CTEQ61 error analysis; the corresponding relative uncertainties are also reported in Fig. 3, which indicates a flat behavior for $M(4\mu) > 150$ GeV. An additional cross check is made in Fig. 4, which reports the comparison between the predictions of CTEQ61 and MRST2001E PDFs.

The effect of μ_F and μ_R variations on $M(4\mu)$ is shown in Fig. 2; one may notice that each of the four different combinations turns out to be dominant as lower (or upper) error boundary in a given $M(4\mu)$ region, with an overall effect which results in flat boundaries. Adopting just μ_F - μ_R correlated variations would underestimate the contribution of QCD scales to the total theoretical uncertainty.

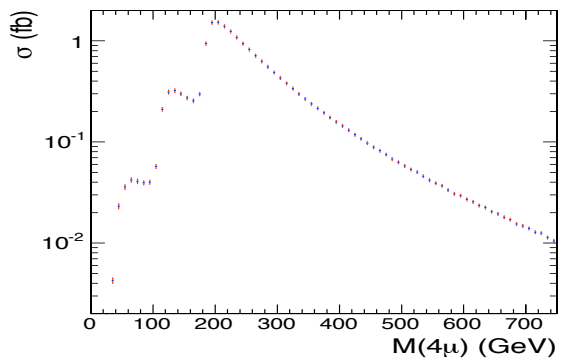

Figure 1: Four muon invariant mass distribution, $\mathrm{M}(4\mu)$, for the process $\mathrm{q\bar{q}} \rightarrow \mathrm{ZZ} \rightarrow 4\mu$ with CTEQ61 PDF and $\mu_\mathrm{F} = \mu_\mathrm{R} = 2\mathrm{M_Z}$. The distribution is normalized to femtobarns per 10 GeV bins. The symmetric error bars result from a full error analysis with the CTEQ61 error sets: they are reported as relative uncertainties in Fig. 3.

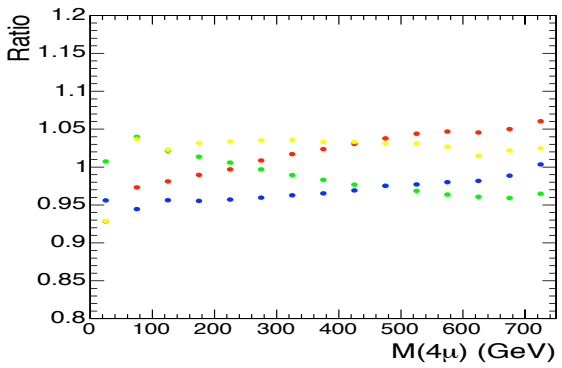

Figure 2: $\mathrm{M}(4\mu)$ distribution according to four different renormalization and factorization scale settings with respect to the reference one ($\mu_\mathrm{F} = \mu_\mathrm{R} = 2\mathrm{M_Z}$): $\mu_\mathrm{F} = \mathrm{M_Z}, \mu_\mathrm{R} = \mathrm{M_Z}$ (red); $\mu_\mathrm{F} = 4\mathrm{M_Z}, \mu_\mathrm{R} = \mathrm{M_Z}$ (yellow); $\mu_\mathrm{F} = \mathrm{M_Z}, \mu_\mathrm{R} = 4\mathrm{M_Z}$ (green); $\mu_\mathrm{F} = 4\mathrm{M_Z}, \mu_\mathrm{R} = 4\mathrm{M_Z}$ (blue).

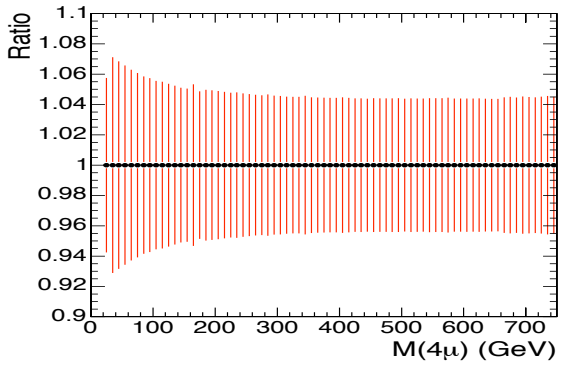

Figure 3: $\mathrm{M}(4\mu)$ distribution: symmetric relative uncertainties from a full error analysis with the CTEQ61 error sets.

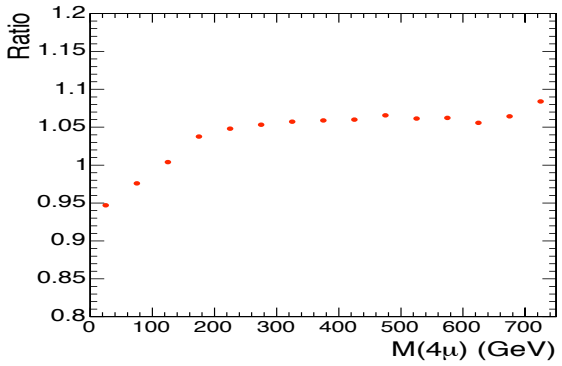

Figure 4: Ratio between $\mathrm{M}(4\mu)$ distributions obtained with the MRST2001 and the CTEQ61 PDFs.

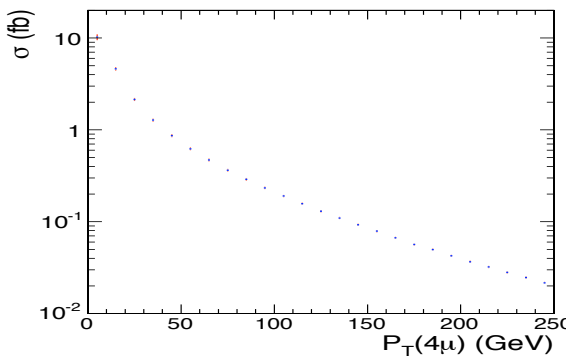

Figure 5: Transverse momentum of the 4μ system, $\mathrm{P_T}(4\mu)$, for the process $\mathrm{q\bar{q}} \to \mathrm{ZZ} \to 4\mu$ with CTEQ61 PDF and $\mu_\mathrm{F} = \mu_\mathrm{R} = 2\mathrm{M_Z}$. The distribution is normalized to femtobarns per 10 GeV bins. The symmetric error bars result from a full error analysis with the CTEQ61 error sets.

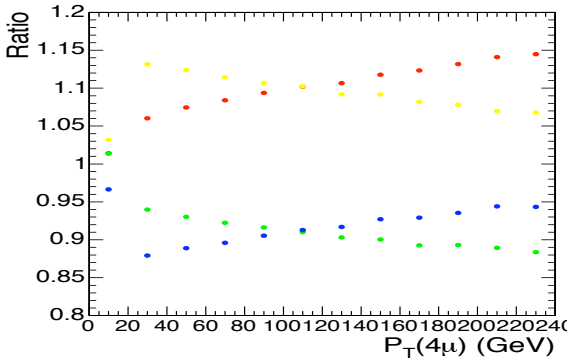

Figure 6: $\mathrm{P_T}(4\mu)$ distribution according to four different renormalization and factorization scale settings with respect to the reference one ($\mu_\mathrm{F} = \mu_\mathrm{R} = 2\mathrm{M_Z}$): $\mu_\mathrm{F} = \mathrm{M_Z}, \mu_\mathrm{R} = \mathrm{M_Z}$ (red); $\mu_\mathrm{F} = 4\mathrm{M_Z}, \mu_\mathrm{R} = \mathrm{M_Z}$ (yellow); $\mu_\mathrm{F} = \mathrm{M_Z}, \mu_\mathrm{R} = 4\mathrm{M_Z}$ (green); $\mu_\mathrm{F} = 4\mathrm{M_Z}, \mu_\mathrm{R} = 4\mathrm{M_Z}$ (blue).

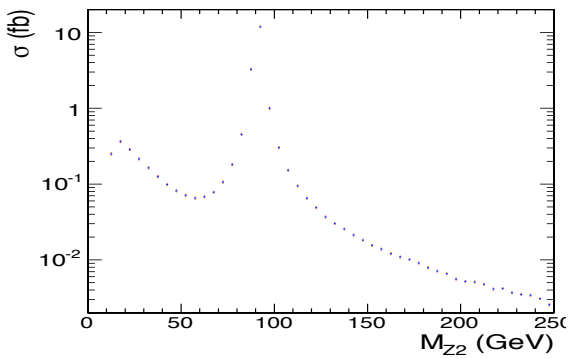

Figure 7: Invariant mass of the Z2 candidate for the process $\mathrm{q\bar{q}} \to \mathrm{ZZ} \to 4\mu$ with the CTEQ61 PDF and $\mu_\mathrm{F} = \mu_\mathrm{R} = 2\mathrm{M_Z}$. The distribution is normalized to femtobarns per 10 GeV bins. The symmetric error bars result from a full error analysis with the CTEQ61 error sets.

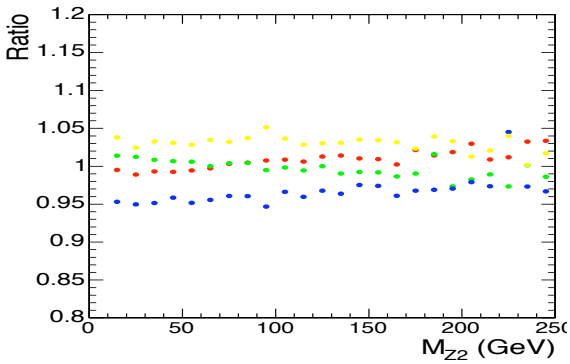

Figure 8: Invariant mass of the Z2 candidate according to four different renormalization and factorization scale settings with respect to the reference one ($\mu_\mathrm{F} = \mu_\mathrm{R} = 2\mathrm{M_Z}$): $\mu_\mathrm{F} = \mathrm{M_Z}, \mu_\mathrm{R} = \mathrm{M_Z}$ (red); $\mu_\mathrm{F} = 4\mathrm{M_Z}, \mu_\mathrm{R} = \mathrm{M_Z}$ (yellow); $\mu_\mathrm{F} = \mathrm{M_Z}, \mu_\mathrm{R} = 4\mathrm{M_Z}$ (green); $\mu_\mathrm{F} = 4\mathrm{M_Z}, \mu_\mathrm{R} = 4\mathrm{M_Z}$ (blue).

All these results are summarized in Table 1. We quote 3-4% effects arising from the variation of the QCD scales and 4-5% effects from CTEQ61 error analysis, while MRST2001 predictions turn out to be consistent with the CTEQ61 ones, with a maximum discrepancy of 1.7σ obtained at $\mathrm{M}(4\mu)$ = 500 GeV (with the "High" Higgs mass selection cuts).

In general, the CTEQ61 error analysis achieves similar results for all the single muon, di-muons and four-muons kinematic distributions in $\mathrm{q\bar{q}} \rightarrow \mathrm{ZZ} \rightarrow 4\mu$ events (4-5% uncertainties with no sensitive dependency on the studied observable). QCD scale variations also achieve similar results for single muon distributions (flat 3-4% effects). However, more sensitive relative uncertainties of up to 10-15% are observed on four-muons and di-muons $\mathrm{P_T}$ and pseudorapidity distributions in $\mathrm{q\bar{q}} \rightarrow \mathrm{ZZ} \rightarrow 4\mu$ events, which suggest to refrain from performing selections based on these observables in the context of Higgs searches.

This is well illustrated in Figs. 5 and 6 which show the $\mathrm{P_T}(4\mu)$ distribution and the corresponding effects of the QCD scales variations, respectively. The effects of the scale variations in the highest statistics bin (for $\mathrm{P_T}(4\mu) < 10$ GeV) turns out to be small, i.e. comparable to the ones observed for single muon distributions. However much larger effects are observed for $\mathrm{P_T}(4\mu) > 10$ GeV.

Fig. 7 reports the invariant mass distribution of the Z2 along with uncertainties from the CTEQ61 error analysis (corresponding to a relative error of around 4% on the overall Z2 mass spectrum), while Fig. 8 shows the effect of μ_F and μ_R variations on the same distribution, which turns out to be more pronounced on the nominal mass of the Z resonance.

5 Normalization to "side-bands" and to Drell-Yan

Normalization to "side-bands" or to higher rate processes involving $q\bar{q}$ initial state provides an experimental methodology to absorb part of the theoretical uncertainties arising from PDF and QCD scales [9].

The sidebands of the $\mathrm{M}(4\mu)$ distribution itself can be used to estimate the background level inside the "signal" $\mathrm{M}(4\mu)$ windows. This method has serious limitations arising from two facts: a rather complex shape of the ZZ background spectrum (with all associated uncertainties) and a relatively low overall statistics. The former suggests one to make sidebands narrower, while the latter naturally asks for wider sidebands. At an integrated luminosity of the order of 30 fb^{-1}, which is a reference value for the Higgs search in the 4μ channel at the LHC, only this second approach is applicable.

As a reference for a high rate process involving a $q\bar{q}$ initial state we consider Z inclusive production with Z bosons decaying to $\mu^+\mu^-$, whose cross section can be measured with systematic errors of around 2% [10], factorizing the larger uncertainties arising from the luminosity measurement.

Single Z boson events decaying to $\mu^+\mu^-$ events are generated with MCFM with pre-selection cuts (applied to di-muons final states) described in section 3 . The total effective cross section $\sigma(\mathrm{p\bar{p}} \rightarrow \mathrm{Z} \rightarrow \mu^+\mu^-)$ turns out to be 924 pb.

Table 2 gives the details of the symmetric PDF and QCD scales uncertainties on the cross section for the $\mathrm{q\bar{q}} \rightarrow \mathrm{ZZ} \rightarrow 4\mu$ process in "signal" regions optimized for the $\mathrm{H} \rightarrow 4\mu$ search [8], along with the corresponding figures for the ratio to the $Z \rightarrow 2\mu$ cross section (ρ_Z) and to the "side-

Table 2: The integrated cross sections for the $\sigma(\mathrm{q\bar{q}} \to \mathrm{ZZ} \to 4\mu)$ process at NLO in different "signal" $\mathrm{M}(4\mu)$ ranges, with the indication of the corresponding applied selection ("P"=Preselection, "L"=Low Mass, "A"=Average Mass, "H"=High Mass), and the figures for symmetric errors from PDF and scale uncertainties (considering the CTEQ61 error sets and the variations of both the factorization and the re-normalization scales (μ_{F}, μ_{R}) between M_Z and $4M_Z$). The ratio ρ_{Z} to the $\mathrm{Z} \to 2\mu$ cross section with symmetric errors from PDF and QCD scale uncertainties. The ratio ρ_{SB} to the ZZ cross section in side bands with symmetric errors from PDF and QCD scales uncertainties. The side-bands are defined in the $\mathrm{M}(4\mu)$ range 100 GeV - 700 GeV excluding the "signal" region.

Range (GeV)	Sel.	σ_{NLO} (fb)	$\Delta\sigma$ pdf	$\Delta\sigma$ μ	ρ_{Z}	$\Delta\rho_{\mathrm{Z}}$ pdf	$\Delta\rho_{\mathrm{Z}}$ μ	ρ_{SB}	$\Delta\rho_{\mathrm{SB}}$ pdf	$\Delta\rho_{\mathrm{SB}}$ μ
113-116	P	0.0670	5.6%	3.9%	7.28E-8	1.1%	0.6%	3.71E-3	2.9%	3.0%
118-121	L	0.0293	5.3%	3.2%	3.21E-8	1.2%	1.9%	1.68E-3	2.6%	2.1%
128-132	L	0.0692	5.3%	3.5%	7.54E-8	1.3%	1.2%	4.08E-3	2.5%	2.3%
138-142	L	0.0795	5.2%	4.1%	8.62E-8	1.4%	1.4%	4.81E-3	2.3%	2.0%
148-152	L	0.0801	5.0%	4.1%	8.71E-8	1.5%	1.8%	4.84E-3	2.1%	1.6%
157-162	L	0.0993	5.0%	4.4%	1.08E-7	1.7%	1.8%	6.02E-3	1.8%	1.6%
167-172	L	0.1130	5.2%	4.7%	1.22E-7	1.9%	2.0%	6.83E-3	1.6%	1.5%
177-182	L	0.2728	5.1%	4.1%	2.95E-7	2.1%	1.8%	1.65E-2	1.2%	1.5%
186-193	A	0.7215	4.9%	3.4%	7.81E-7	2.2%	1.7%	5.49E-2	1.1%	1.6%
195-203	A	1.1189	4.9%	3.5%	1.24E-6	2.3%	1.9%	8.73E-2	1.0%	1.4%
241-257	A	1.1880	4.7%	3.7%	1.29E-6	3.1%	3.1%	9.37E-2	0.2%	0.2%
287-311	A	0.8901	4.6%	3.6%	9.63E-7	3.6%	4.0%	6.86E-2	0.6%	0.8%
329-369	A	0.8131	4.5%	3.4%	8.80E-7	4.1%	4.7%	6.23E-2	1.2%	1.6%
364-428	H	0.3736	4.3%	3.3%	4.04E-7	4.5%	5.4%	7.26E-2	1.6%	2.2%
394-494	H	0.4043	4.3%	3.3%	4.38E-7	4.8%	5.9%	7.90E-2	2.0%	2.8%
417-561	H	0.4282	4.3%	3.3%	4.63E-7	5.0%	6.3%	8.41E-2	2.3%	3.2%
438-650	H	0.4524	4.2%	3.7%	4.90E-7	5.3%	6.7%	8.93E-2	2.6%	3.6%
453-697	H	0.4351	4.2%	3.9%	4.71E-7	5.4%	6.9%	8.55E-2	2.8%	3.8%

bands" (ρ_{SB}). The "side-bands" are defined in the $\mathrm{M}(4\mu)$ range 100 GeV - 700 GeV excluding the "signal" region.

Fig. 9 shows the comparison between the predictions for $\sigma(\mathrm{q\bar{q}} \to \mathrm{ZZ} \to 4\mu)$ and ρ_Z in the $\mathrm{M}(4\mu)$ range 195 - 203 GeV, according to the 40 CTEQ61 error sets (with central value normalized to the prediction of the reference CTEQ61 set). A significant fraction of $\sigma(\mathrm{q\bar{q}} \to \mathrm{ZZ} \to 4\mu)$ variation in this "signal" range is due to the CTEQ61 eigenvector (19,20), and turns out to be absorbed in the ratio to $\sigma(\mathrm{p\bar{p}} \to \mathrm{Z} \to 2\mu)$. Instead, an anti-correlation effect between the two processes shows up for the eigenvector (9,10), which dominates the total PDF error on ρ_Z.

Fig. 10 shows the comparison between the predictions for $\sigma(\mathrm{q\bar{q}} \to \mathrm{ZZ} \to 4\mu)$ and ρ_{SB} in the $\mathrm{M}(4\mu)$ range 195 - 203 GeV, according to the 40 error members of CTEQ61 (central value normalized to the reference CTEQ61 set). A strong correlation between cross sections in "signal" and "side-band" regions is observed for all the CTEQ61 eigenvectors. Indeed, this is compatible with the figure reported in Table 2, which gives 1% for the PDF uncertainty on ρ_{SB} in this $\mathrm{M}(4\mu)$ range.

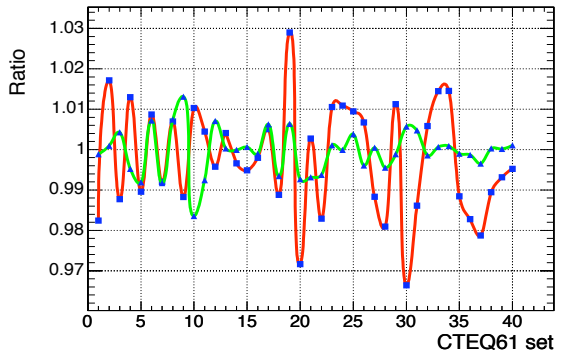

Figure 9: Residuals obtained with the 40 members of the CTEQ61 sets for the cross section of the process $q\bar{q} \rightarrow ZZ \rightarrow 4\mu$ (red line, squares) and for the ratio between $q\bar{q} \rightarrow ZZ \rightarrow 4\mu$ and $p\bar{p} \rightarrow Z \rightarrow 2\mu$ cross sections (green line, triangles) in the $M(4\mu)$ range 195 - 203 GeV.

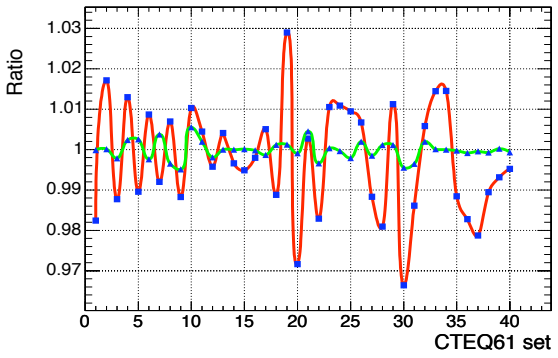

Figure 10: Residuals obtained with the 40 members of the CTEQ61 sets for the cross section of the process $q\bar{q} \rightarrow ZZ \rightarrow 4\mu$ (red line, squares) and for the ratio between the cross sections in "signal" and "side-band" regions (green line, triangles), quoted in the $M(4\mu)$ range 195 - 203 GeV.

The qualitative evaluation from visual inspection of Fig. 9 and Fig. 10 corroborates the assumption of symmetric errors, which turns out to be particularly convenient in significance estimators [8]. In order to quantify the differences between the PDF uncertainty figures quoted with symmetric errors and those quoted with asymmetric errors, we concentrate on the error analysis for the $M(4\mu)$ range 195 - 203 GeV. An asymmetric error analysis in this range gives the results summarized in Table 3, which are in agreement with the symmetric errors reported in Table 2 for the same range.

Table 3: The integrated cross section for the $\sigma(q\bar{q} \rightarrow ZZ \rightarrow 4\mu)$ process at NLO with average mass selection cuts in the $M(4\mu)$ range 195 - 203 GeV along with the figures for the asymmetric errors from PDF uncertainties (considering the CTEQ61 error sets). The ratio ρ_Z to the $Z \rightarrow 2\mu$ cross section along with the asymmetric errors from PDF uncertainties. The Ratio ρ_{SB} to the ZZ cross section in side bands along with the asymmetric errors from PDF uncertainties. The side bands are defined in the $M(4\mu)$ range 100 GeV - 700 GeV excluding the "signal" region.

Range (GeV)	σ_{NLO} (fb)	$\Delta^-\sigma$ pdf	$\Delta^+\sigma$ pdf	ρ_Z	$\Delta^-\rho_Z$ pdf	$\Delta^+\rho_Z$ pdf	ρ_{SB}	$\Delta^-\rho_{SB}$ pdf	$\Delta^+\rho_{SB}$ pdf
195-203	1.1189	5.4%	4.3%	1.24E-6	2.6%	2.1%	8.73E-2	1.0%	0.9%

Fig. 11 gives the total (squared sum) uncertainties from PDF and QCD scales on the absolute cross section, ρ_Z and ρ_{SB} in "signal" ranges. The total uncertainty on the absolute cross section is basically flat, oscillating between 6% and 7% from 100 to 200 GeV, and smoothly decreasing to 5.5% at high $M(4\mu)$.

The total theoretical uncertainty on ρ_{SB} is lower than 4.5% in the overall $M(4\mu)$ range, and becomes very small (less than 2.5%) between 160 and 350 GeV, making the normalization to "side-bands" particularly convenient at average $M(4\mu)$, i.e. on the peak of the $M(4\mu)$ distri-

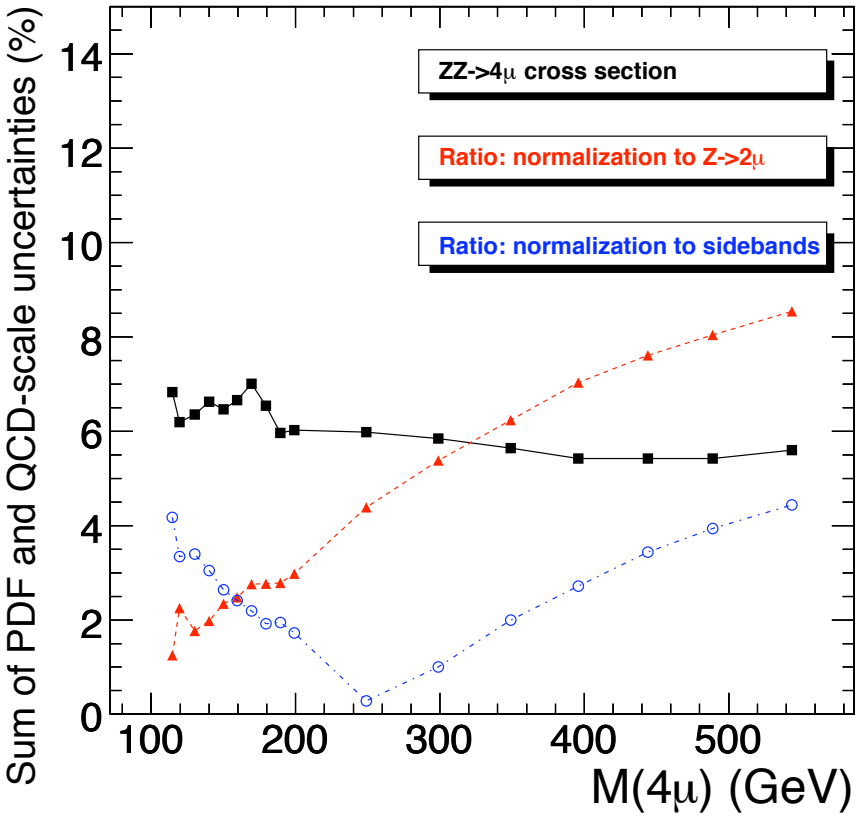

Figure 11: Total (squared sum) uncertainties from PDF and QCD scales for the $\sigma(q\bar{q} \to ZZ \to 4\mu)$ process at NLO (black squares), ratio to the cross section in side bands (blue circles) and ratio to the $p\bar{p} \to Z \to 2\mu$ cross section (red triangles) in different "signal" $M(4\mu)$ ranges (see Table 2). Side bands are defined in the $M(4\mu)$ range 100 - 700 GeV excluding the "signal" region.

bution. However, one should take into account that with 30 fb^{-1} of integrated luminosity, the typical statistical error on the events collected in side-bands will be 5%. Since this figure is scaling down with the square root of the integrated luminosity, in order to appreciate normalization precisions at the 2% level it will be necessary to collect at least 300 fb^{-1} of integrated luminosity.

The total theoretical uncertainty on ρ_Z smoothly increases with $M(4\mu)$, staying below the 3% threshold for $M(4\mu)$ up to 200 GeV. Thanks to the high rate of the $Z \to 2\mu$ process, one can get negligible statistical contributions to $\Delta\rho_Z$ with integrated luminosities below 1fb^{-1}. Above 300 GeV, the total relative error curve for ρ_Z crosses the corresponding one on the total cross section. However, in order to estimate the cross section of the $q\bar{q} \to ZZ \to 4\mu$ process, normalization to the $Z \to 2\mu$ process might be convenient even above 300 GeV, considering the advantage of absorbing the error for the luminosity measurements. Effects of these theoretical uncertainties on significance estimators for the $H \to 4\mu$ mass dependent search are reported in reference [8].

One of the main limitations of these normalization methodologies arise from the fact that this study doesn't take into account electroweak corrections. Such corrections should mostly affect

the normalization in the high $\mathrm{M}(4\mu)$ range. The effects of the complete logarithmic electroweak $O(\alpha)$ corrections on the production of vector-boson pairs at the LHC have been studied in [11]. These corrections turn out to be relevant for $M(4\mu)$ of the order of several 100 GeV lowering the Born level predictions by more than 10% for $M(4\mu) > 500$ GeV.

Although the size of these corrections turns out to be similar for single and double boson production [11, 12], corrections to the ratio of the corresponding cross sections might be sensitive in the high $\mathrm{M}(4\mu)$ region.

6 Conclusions

The effects of the theoretical uncertainties from PDF and from renormalization and factorization scales are studied for the $\mathrm{q\bar{q}} \rightarrow \mathrm{ZZ} \rightarrow 4\mu$ process at NLO using MCFM.

The CTEQ61 error analysis achieves flat 4-5% uncertainties for all the single muon, di-muons and four-muons kinematic distributions.

Independent variations of the renormalization and factorization scales also achieve similar results for single muon distributions (convolution resulting in flat 3-4% uncertainties). However, more sensitive relative uncertainties of up to 10-15% are observed on four-muons and di-muons $\mathrm{P_T}$ and pseudorapidity distributions.

Normalization to Drell-Yan processes with di-muon final states (ρ_Z) and/or to side-bands (ρ_{SB}) provide an experimental methodology to absorb part of the theoretical uncertainties arising from PDF and QCD scales, factorizing at the same time the larger uncertainties from the luminosity measurement.

Given the high rate of the process, normalization to Drell-Yan is particularly convenient at low integrated luminosities. The total theoretical uncertainty on ρ_Z turns out to be below 2.5% in the low $M(4\mu)$ range (between 100 and 160 GeV).

Normalization to side-bands, instead, is applicable only at high integrated luminosities, well above 30 fb^{-1} . Neglecting the statistical contribution, the total theoretical uncertainty on ρ_{SB} turns out to be lower than 4.5% in the overall $M(4\mu)$ range, and becomes very small (less than 2.5%) between 160 and 350 GeV.

7 Acknowledgments

We would like to thank M. Aldaya, P. Arce, A. Ballestrero, D. Bourilkov, J. Caballero, J. Campbell, B. Cruz, G. Dissertori, S. Ferrag, U. Gasparini, P. Garcia, J. Hernandez, I. Josa, E.R. Morales, N. Neumeister, A. Nikitenko and T. Sjöstrand for their active participation in the analysis discussions and comments on this note.

References

[1] P. Bartalini, R. Chierici, and A. De Roeck,. CERN-CMS-NOTE-2005-013.

[2] J. M. Campbell and R. K. Ellis, `http://mcfm.fnal.gov`.

[3] W. Giele and M. R. Whalley, http://durpdg.dur.ac.uk/lhapdf/.

[4] D. Stump *et. al.*, *JHEP* **10** (2003) 046, [hep-ph/0303013].

[5] J. Pumplin *et. al.*, *Phys. Rev.* **D65** (2002) 014013, [hep-ph/0101032].

[6] A. D. Martin, R. G. Roberts, W. J. Stirling, and R. S. Thorne, *Eur. Phys. J.* **C28** (2003) 455–473, [hep-ph/0211080].

[7] R. W. L. Jones, M. Ford, G. P. Salam, H. Stenzel, and D. Wicke, *JHEP* **12** (2003) 007, [hep-ph/0312016].

[8] A. Drozdetskiy *et. al.*,. CERN-CMS-NOTE-2006-122.

[9] M. Dittmar, F. Pauss, and D. Zurcher, *Phys. Rev.* **D56** (1997) 7284–7290, [hep-ex/9705004].

[10] J. Alcaraz,. CERN-CMS-NOTE-2006-082.

[11] E. Accomando, A. Denner, and A. Kaiser, *Nucl. Phys.* **B706** (2005) 325–371, [hep-ph/0409247].

[12] E. Accomando, A. Denner, and C. Meier, hep-ph/0509234.